MINERALOGICAL REPORT No. 8522

by Alan C. Purvis, PhD

June 21st, 2004

TO :	Arafura Resources NL 6 Porter Street DARWIN NT 0820 Attention: Mr John Goulevitch
YOUR REFERENCE :	Order No. 0047
MATERIAL :	Rock samples, Arunta Inlier, 11 in all
IDENTIFICATION :	L1/1-3, HB, HC, H/D/1 and 4; H/E/1 and 4, H/F/1 and 3
WORK REQUESTED :	Polished thin section preparation, petrological/mineragraphic descriptions and report. Electron microprobe analysis as required.
SAMPLES & SECTIONS :	Returned to you with this report.
DIGITAL COPY :	Enclosed with hard copy of this report.

PONTIFEX & ASSOCIATES PTY. LTD.

CONTENTS

SUMMARY COMMENTS: Optical Microscopy

SUMMARY AND DISCUSSION: Electron Microprobe Analysis of REE

Table 1: Microprobe analyses REE bearing minerals
Table 2: Reconstruction of florencite compositions sample H/D/1
Figure 1: Monazite (HF-3) Rhabdophane (HD-4) normalised to Primitive Mantle
Figure 2: REE patterns for six florencite-crandallite-plumbogummite analyses, H/D/1
Figure 3: Sample HE-1. Apatite (pt 1) and Ce4+ (pt2), normalised to Primitive Mantle.

COMMENTS on Genesis of REE-rich "H-Series" Samples

INDIVIDUAL PETROGRAPHIC DESCRIPTIONS with integrated photomicrographs Fig 1 to Fig 13 (for sections analysed by microprobe).

SUMMARY COMMENTS: OPTICAL MICROSCOPY

Eleven samples from two prospects in the Arunta Inlier (N.T.) are described in this report from polished thin sections as requested. It is understood that REE content is of particular interest and for this reason, four of these sections were also investigated by electron microprobe at "Adelaide Microscopy", University of Adelaide (as agreed with John Goulavitch, pers comm) and selected photomicrographs of appropriate phases are integrated with the descriptions.

The sample numbers, their essential petrographic characteristics, including minor and likely REE minerals, as initially assessed by optical microscopy are listed below. [Results of electron microprobe analyses and discussion on REE then follow.]

L1/1	Calc-silicate, abundant amphibole. Possible metadolomitic sandstone
L1/2	Evolved monzogranite or muscovite-rich pegmatite. Accessory garnet, strong foliation.
L1/3	Calc-silicate, abundant clinopyroxene. Possible meta-dolomitic sandstone
H/B	Heterogeneous limonite-stained cherty/microsparry quartz, with hematite, barite, accessory monazite and/or xenotime
H/C	Barite-rich with hematite, clay-limonite, minor monazite (or xenotime)
**H/D/1	Massive quartz, subordinate coarse barite, altered biotite. Minor alunite-like mineral, rare monazite xenotime.
**H/D/4	Coarse quartzose rock with fine grained quartz, ?kaolinite and hematite, small spherulites of uncertain composition but checked by probe as possibly alunite-related. Single grain of monazite?
**H/E/1	Heterogeneous quartz-kaolinite (?)-limonite rock. Minor apatite and rarer barite. (Rare grains with Ce indicated by probe).
H/E/4	Heterogeneous quartz-barite-limonite rock. Accessory apatite, pyrite, rare monazite/xenotime.
H/F/1	Quartz-limonite rock with rare goethite, monazite, gradational into anastomosing to lamellar limonitic kaolinite, quartz chalcedony, accessory monazite/xenotime, layers of barite.
**H/F/3	Heterogeneous aggregate of dominant barite, subordinate quartz, kaolinite, muscovite, local hematite and monazite.

Samples annotated ** investigated by electron-microprobe.

SUMMARY AND DISCUSSION : ELECTRON MICROPROBE ANALYSIS REE

As indicated, microprobe analyses were carried out on four selected samples annotated by ** above at "Adelaide Microscopy", University of Adelaide, by their operator using a high power beam to detect REE, and as personally directed by this author Alan Purvis.

A major aim of this probe work was to investigate examples of the monazite-cheralite-group REE minerals, or xenotime, in four sections, as seen by the optical microscopy discussed above, but generally not possible to positively identify in thin section. The same or similar/related accessory phases in other polished thin sections were not analysed by microprobe, therefore this investigation is not claiming to be an exhaustive assessment of REE representation within the whole suite.

The probe also analysed an optically alunite-like mineral in H/D/1, possibly with REE and P substituting potassium and sulphur in the alunite structure. [The formulae for alunite is $KAl_3(SO_4)_2(OH)_6$, compared to $CeAl_3(PO_4)_2(OH)_6$ for florencite.] As noted below however, florencite grains were adversely affected by the high beam current, and therefore give poor totals compared to those expected from assumed water content.

Barite in two samples was investigated but REE was found to be absent. Texturally distinctive spherulites in H/D/4 were checked for REE, but again found to be absent.

Table 1 presents analyses of the several REE-bearing phases investigated in the four selected polished thin sections. Some of these phases are well defined, including apatite, monazite and rhabdophane identified in several samples. Others are poorly defined, with Ce^{4+} minerals and apparently florencite-rich members of the crandallite group in the alunite family. REE patterns shown in Figs 1-3 are normalised against primitive mantle values, which are about 2.1 times chondritic values more usually applied, but mantle and chondrite-normalised patterns are parallel to each other.

The spherulites in sample H/D/4 were found to contain only Fe, Al, Si and O (± H) and do not contain REE. A single grain of rhabdophane [$(Ce,La)PO_4.nH2O$] was identified in this sample however.

Monazite was identified in H/F/3, which has low Th, Ca and Si and low contents of $CaTh(PO_4)_2$ (brabantite) and $ThSiO_4$ (huttonite) components. Cheralite, as seen in apatite-

rich samples from this area, is a solid solution with 20-80% brabantite as well as monazite,

and as much as 1/3 huttonite, but is not present in these samples. The rhabdophane (equivalent to monazite + water) has a strong negative Ce anomaly but higher middle REE than the monazite (Fig. 1), which has unusual REE patterns, including very low Gd but higher Dy and Er.

Analysis of florencite-rich phases in H/D/1 was complicated by reaction with the high-energy beam used to measure REE. For this reason some values, giving rise to spiky REE patterns, may be incorrect or at least suspect. The crystals are clearly zoned with higher mean atomic numbers (and REE contents) in cores compared to rims. Low totals and unresolvable element ratios suggest that damage due to high currents has resulted in low values for elements other than Al. Both analyses have steeply rising patterns from Y to Er, consistent with the monazite patterns. Reconstructed compositions (Table 2) show 27-30% crandallite as well as 70-73% florencite in solid solution.

Analyses of apatite and a bright Ce-rich phase in H/E/1 both have increasing heavy REE from Dy to Er, but the Ce phase, which has a very strong positive Ce anomaly, would seem to have mostly tetravalent cerium. Apart from Ce, this has Si and P as well as less abundant Al, Pb, Th and Ca. Other rare earths are more abundant in the bright Ce-rich phase (11.8%), than in the apatite (~1% total REE).

No REE were recorded in any of the several checks on barite.

REFERENCE

HANS-JÜRGEN FÖRSTER: 1998 The chemical composition of REE-Y-Th-U-rich accessory minerals in peraluminous granites of the Erzgebirge-Fichtelgebirge region, Germany, Part I: The monazite-(Ce)-brabantite solid solution series. *American Mineralogist, Volume 83, pages 259–272*

Table 1: Microprobe analyses of REE-bearing minerals for Arafura Resources, Report No 8522

	HE1 pt 1	*HE1 pt 2 (bright)*	*HF-3 C1 pt 1*	*HF-3 C1 pt 2*	*HD-4 c1 pt1*
	Apatite	*Unknown*	*Monazite*	*Monazite*	*Rhabdophane*
Al_2O_3	0.00	2.00	0.00	0.02	0.50
SiO_2	0.49	11.36	3.06	3.24	0.61
P_2O_5	40.42	20.10	21.74	21.77	25.15
SO_3	n.d.	n.d.	0.43	0.43	0.00
CaO	57.99	3.67	0.37	0.55	2.68
Y_2O_3	0.10	0.42	0.03	0.02	0.19
La_2O_3	0.06	0.42	19.11	20.42	23.78
Ce_2O_3	0.29	4.75	36.07	34.70	2.53
CeO_2	n.c.	52.59	n.c.	n.c.	n.c.
Pr_2O_3	0.01	0.17	2.56	2.33	6.25
Nd_2O_3	0.40	0.91	7.53	6.62	25.07
Sm_2O_3	0.11	0.28	0.27	0.12	2.67
Gd_2O_3	0.04	0.19	0.00	0.00	0.65
Dy_2O_3	0.00	0.04	0.00	0.05	0.02
Er_2O_3	0.07	0.14	0.09	0.04	0.01
PbO	0.02	1.80	0.15	0.19	0.02
ThO_2	0.00	1.01	8.33	9.33	0.83
UO_2	0.00	0.16	0.25	0.19	0.08
	100.00	100.00	100.00	100.00	91.05

Note: n.d. means not determined:
n.c. means not calculated.

Table 2: Reconstructions of the florencite compositions Sample H/D.1:

	1	*2*	*3*	*4*	*Bright zones*	*Dark zone*
SiO_2	0.14	0.48	0.10	0.09	0.09	0.05
Al_2O_3	31.07	30.97	31.12	30.89	31.60	31.53
P_2O_5	26.11	25.89	26.20	26.26	27.21	27.34
SO_3	1.16	1.03	1.15	1.04	0.91	0.84
CaO	2.40	2.43	3.06	2.89	3.12	3.41
PbO	2.48	3.61	5.81	6.89	0.75	4.45
ThO_2	0.16	0.11	0.10	0.10	0.08	0.10
UO_2	0.04	0.04	0.08	0.02	0.06	0.00
La_2O_3	6.48	6.30	5.16	4.47	8.63	4.11
Ce_2O_3	12.29	11.57	9.69	9.74	12.46	10.40
Pr_2O_3	1.35	1.36	0.91	0.91	0.77	0.82
Nd_2O_3	3.68	3.59	3.76	3.76	2.01	4.01
Sm_2O_3	0.35	0.35	0.54	0.45	0.30	0.49
Gd_2O_3	0.29	0.26	0.08	0.17	0.06	0.25
Dy_2O_3	0.02	0.07	0.00	0.08	0.11	0.00
Y_2O_3	0.18	0.20	0.20	0.22	0.08	0.18
Er_2O_3	0.02	0.00	0.03	0.08	0.01	0.26
	88.22	88.26	87.99	88.06	88.25	88.24

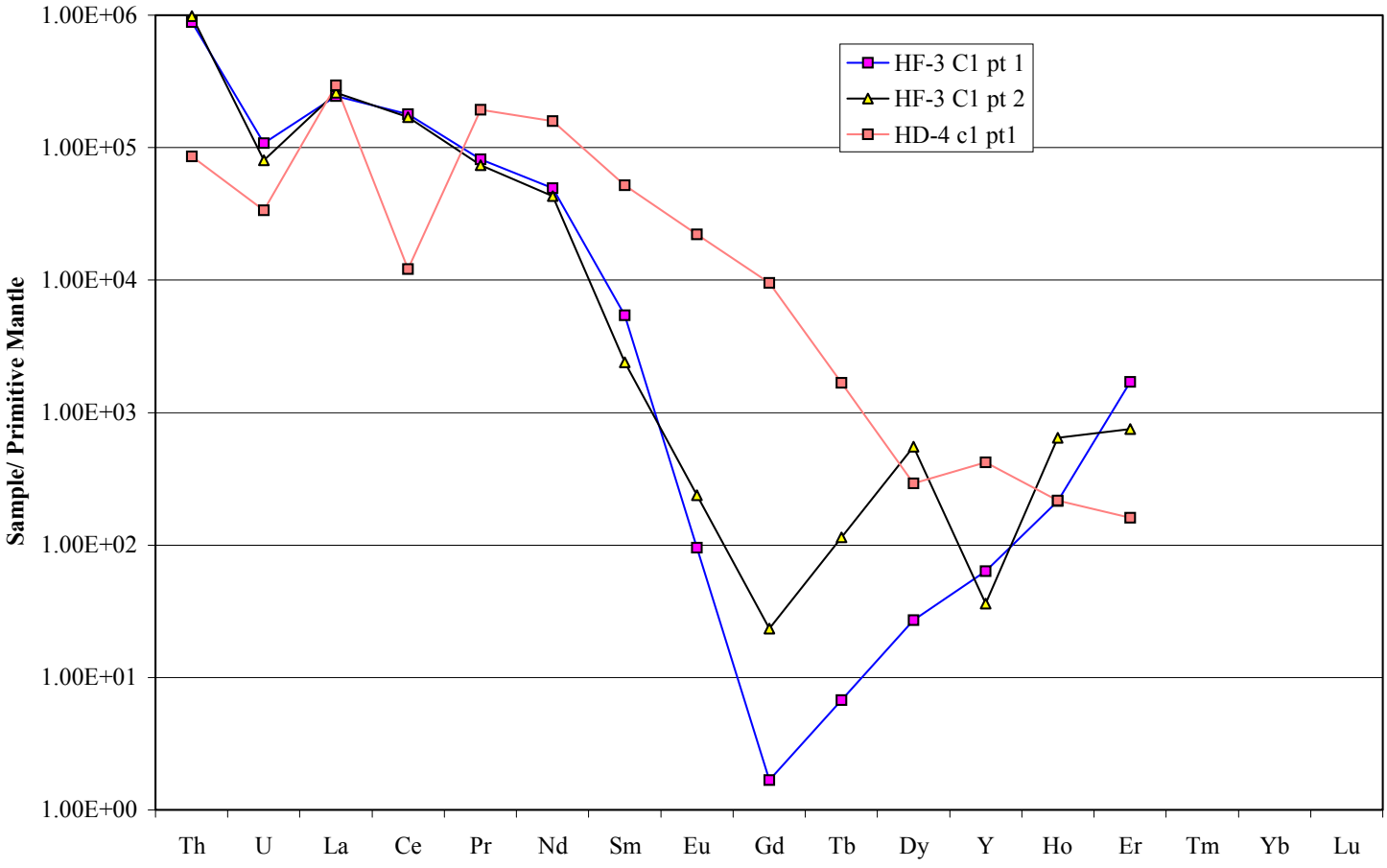

Fig 1: Monazite (HF-3) and Rhabdophane (HD-4) normalised to Primitive Mantle

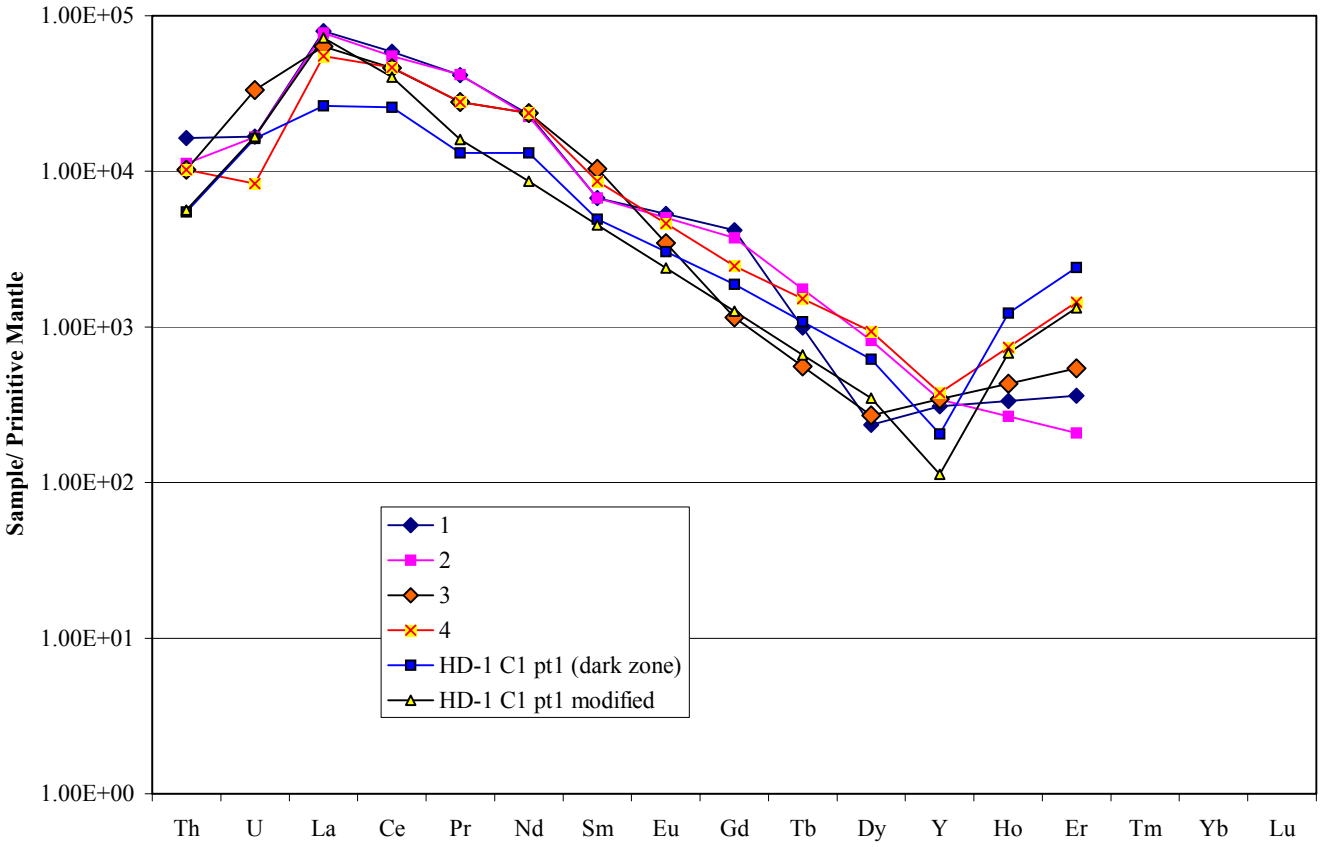

Figure 2: REE patterns for six florencite-crandallite-plumbogummite analyses HD-1.

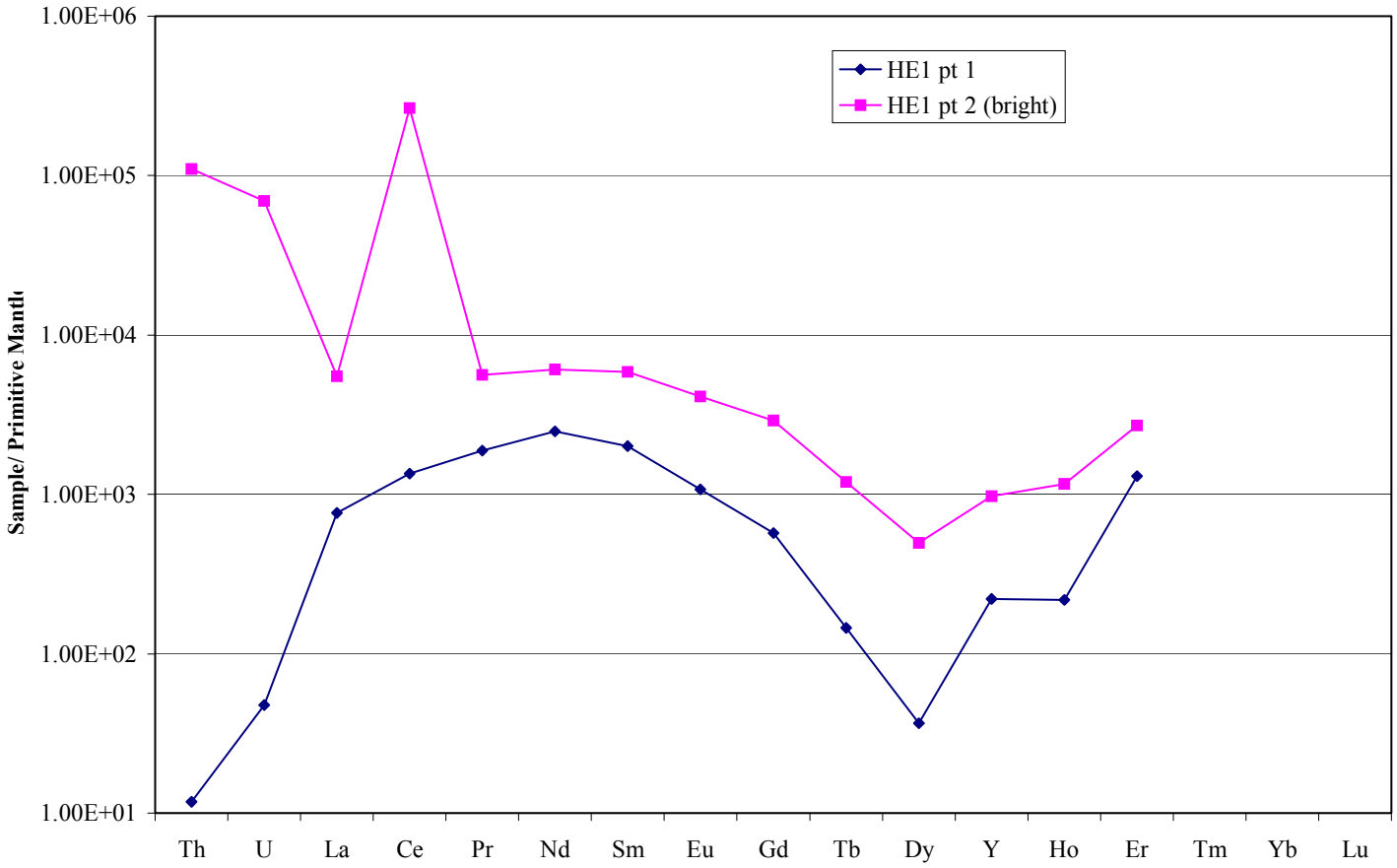

Fig 3: Sample HE-1, Apatite (pt1), and Ce^{4+}-rich phase (pt2) normalised to Primitive Mantle

COMMENTS ON GENESIS OF REE-RICH "H-Series" SAMPLES

The 'H-series' samples are dominated by irregular areas of variably cryptocrystalline, fine sparry silica which may be supergene or possibly of other low temperature genesis together with clays and limonite. Monazite in several samples is the most clearly primary mineral, apart from coarse apatite in H/E/1 and probably the hematite in some samples, particularly H/F/3. Other supergene minerals include florencite-crandallite-plumbogummite crystals in H/D/1, and unidentified spherulites in H/D/4. It is not clear whether barite and locally developed interstitial quartz in various samples are residual primary minerals or partly supergene. Some of these are interstitial to supergene minerals, but it is possible that the supergene minerals have replaced former primary phases and that the barite and quartz were originally interstitial to those minerals. Supergene silica also cuts across individual monazite grains, as seen in Fig. 9, sample H/F/3. Strong oxidation has clearly affected some of the supergene minerals, with a negative Ce anomaly in rhabdophane in H/D/4 indicating that >90% of the Ce is Ce4+.

An unusual characteristic of the monazite in sample H/F/3 is the steeply rising heavy REE patterns, not seen in the rhabdophane in sample H/D/4, but to some extent reflected in the florencite in H/D/1 and the apatite in H/E/1. REE patterns with rising values from Gd to Yb are seen in some evolved, mostly high-temperature granitoids (e.g. 'A-types') and are possible in related pegmatites. This may suggest that the original lithology could represent evolved phosphatic pegmatites, with possibly elevated Ba in alkali feldspar, remobilised into barite during weathering or alteration, or hydrothermal veins with primary barite and rare primary quartz.

The lack of evidence for high Sr in apatite or in florencite would seem unfavourable to any suggestion that these samples could be related to carbonatite, for example, as apatite in carbonatites has commonly over 1% Sr). Strong oxidation has clearly affected some of the supergene minerals, with a negative Ce anomaly in rhabdophane in H/D/4 indicating that >90% of the Ce is $Cr^{4+.}$

INDIVIDUAL PETROGRAPHIC DESCRIPTIONS

L1/1 **Quartz-amphibole-epidote-plagioclase-titanite calc-silicate possibly derived from a dolomitic sandstone.**

This is a heterogeneous rock with greenish-grey and white areas. The thin section contains about 55% quartz, 35% green amphibole, possibly actinolite or hornblende, 5% epidote, 4-5% calcic plagioclase and minor titanite (sphene). The plagioclase is possibly bytownite or anorthite.

Quartz as the main mineral occurs in layers and lenses to 7mm wide, with less abundant amphibole, epidote and plagioclase, but most of the thin section has more abundant amphibole. In the quartz-rich areas the quartz is as much as 5mm in grainsize, with plagioclase to 2mm but mostly smaller grains of epidote and plagioclase. The amphibole-rich areas contain large poikiloblastic grains, one of which is at least 20mm long and 10mm wide, as well as smaller anhedral, partly poikiloblastic grains, enclosing abundant quartz as well as plagioclase and epidote. The larger amphibole grains are elongate parallel to the layering defined by the most quartz-rich lens, and the other grains are also at a low angle to the layering, suggesting a weak foliation. Minor titanite is disseminated through these areas and there is rare chlorite, enclosed within amphibole and possibly of retrograde origin. One epidote grain has a core of altered possible allanite.

This sample is a quartz-rich calc-silicate and may represent a dolomitic sandstone with some detrital titanium minerals now represented by titanite. Clays with aluminium have given rise to epidote and plagioclase. The epidote is pale coloured and probably iron-poor and the plagioclase seems to be poor in sodium. Amphibolite-facies metamorphism is indicated, but possibly less than about 650°C.

L1/2 **Evolved monzogranite or muscovite-rich pegmatite, with accessory garnet and a strong foliation.**

There is a strong foliation in this sample, defined by abundant commonly oriented muscovite. The visually estimated mineralogy includes 35% quartz, 25% microcline, 20-25% muscovite and 15-20% plagioclase, together with about 0.5% garnet. The quartz and feldspar grains are anhedral, with feldspars mostly less than 2mm in grainsize, but some poikilitic grains of quartz to 6mm long. The muscovite is largely schistose and less than 2mm in grainsize, but there are some decussate aggregates. Subhedral garnet crystals about 2mm in diameter are present, with large inclusions of quartz.

This sample is interpreted to represent a highly evolved granitoid (monzogranite) or a micaceous facies of fine-grained pegmatite, with possibly manganese-rich garnet as an accessory. The foliation is probably tectonic and the abundant muscovite suggests low temperatures, again below about 600-650°C, depending on the pressure.

L1/3 **Quartz-clinopyroxene-epidote-amphibole-plagioclase-titanite calc-silicate. Interpreted as a metamorphosed dolomitic sandstone.**

This is a calc-silicate comparable with L1/1, but is less quartz-rich and also has less amphibole. The visually estimated mineralogy includes 35-40% quartz, 35-40% clinopyroxene, 15% epidote, 5% tremolite-actinolite and 2% plagioclase, as well as possibly 2% titanite (sphene). In some quartz-rich areas there are quartz grains more than 2mm in diameter, and both epidote and clinopyroxene include poikiloblastic grains to 3 or 4mm in diameter, enclosing quartz, amphibole, or clinopyroxene (in epidote). Smaller grains of quartz, epidote, clinopyroxene and amphibole also occur, as well as very minor calcic plagioclase, also seen in L1/1. There is more abundant titanite in this sample compared to L1/1, and a more carbonate-rich protolith is suggested by smaller abundance of quartz.

The metamorphism was apparently of the same grade as the previous samples, but this sample is not foliated, possibly reflecting the abundance of clinopyroxene.

H/B **Heterogeneous aggregate of limonite-stained cherty to microsparry quartz with subordinate barite, lesser hematite ± limonite and accessory very minor monazite and/or xenotime.**

Irregular masses of hematite occur in this sample (~7-8%), partly granular with a mosaic texture but partly more heterogeneous with crystalline and earthy hematite as well as limonite. These masses are as much as 8mm long and are enclosed in a heterogeneous but mostly quartz-rich matrix. Various domains of microcrystalline (cherty) to microsparry quartz are abundant and are irregularly stained by limonite. Irregular limonitised or leached patches also occur, usually with microgranular quartz, and there are also leached voids to 4mm long. Sparsely disseminated larger grains of earlier, deformed and polygonised quartz occur to 1.5mm in grainsize, but large rounded or slightly irregular grains of barite, to 6mm in diameter, are more abundant (~20%).

Sparse small polycrystalline aggregates seem to consist of monazite or xenotime, <1%. These grains seem to be uniaxial, therefore xenotime is possible since, although the 2V of monazite is very small (as little as 6°), it is usually detectible. (The same or similar phases are more abundant in other samples in this suite.)

H/C **Barite-rich rock with hematite, clay-limonite lenses, minor quartz and disseminated monazite/xenotime (?).**

This hand specimen is dominated by pale pinkish barite with fractured and fragmented masses of hematite to 10mm in diameter and limonite-stained zones. In the thin section the barite (possibly >80%) is seen to be inequigranular with slightly strained old grains to 15mm long as well as abundant smaller possibly recrystallised new grains. Irregular limonite to clay-rich lenses are common (possibly as much as 10%) and partly stylolitic, locally passing into minor fine-grained quartz (totalling less than 5%), as small lenses and also possibly replacing, and enclosing residual kernels of barite in some areas.

The hematite masses (3-4%) are irregular and are fractured with limonite-stained clays, but also contain lenses of fine-grained monazite/xenotime as seen in the other samples. Scattered single grains and lenticular aggregates of the same mineral are reasonably abundant compared to the previous sample, possibly more than 5% of the thin section, with crystals to 0.5mm long. Some of the crystals have inclined extinction, favouring monazite over xenotime.

H/D/1** **Limonite-stained quartz-rich mass with coarse-grained barite, lamellar kaolin-limonite-leucoxene possibly ex biotite. Local lenses of a possible alunite-like mineral and rare monazite/xenotime. [Identified by probe analysis as florencite with minor crandallite and plumbogummite.**

** indicates selected points analysed in this polished thin section by electron microprobe.

There is less abundant barite in this sample compared to the previous sample, possibly 15-20% by volume, in a quartz-rich matrix with relatively sparse monazite or xenotime. The host has abundant larger grains and prisms of quartz, to 1mm long, with zones outlined by fluid-inclusions, in microcrystalline quartz usually stained with limonite. Patches of fibrous quartz are also common and seem to be of low-temperature hydrothermal origin. A lens rich in kaolinite, with lamellar limonite and leucoxene, occurs adjacent to the main area of lamellar quartz and may indicate the presence of biotite or phlogopite in the protolith. The barite grains are as much as 15mm long and contain lamellae defined by disseminated small elongate quartz grains and prisms, or more continuous fractures filled with microsparry quartz. Irregular, partly stylolite-like clay-limonite masses occur, as in the previous samples, but are less abundant, and are accompanied by irregular masses of heavily limonite-stained quartz.

Adjacent to some of the limonite-quartz masses are minor lenses rich in small rhombohedral crystals of a probable alunite-group mineral (3-4%), possibly rich in REE and P. Some areas seem to have a higher birefringence than florencite, but other lenses, to 5 x 3mm, seem to have lower birefringences. Rare (<1%) very small grains and aggregates of monazite/xenotime are present.

Figs 1 & 2 **H/D/1** **0.18 mm**

TS. Fig 1: Plane polarised light (PPL), Fig 2: Crossed nicols (Xnic). Large areas of interstitial barite ("dusty" and high relief in Fig 1) and a central irregular crystal of fractured monazite or rhabdophane (coloured in Fig 2). Irregularly limonite stained quartz widespread and best seen in Fig. 1, to form about 2/3 of the photo.

Figs 3 & 4 **H/D/1** 0.45 mm

TS. Fig 3: PPL. Fig 4: Xnic. Irregular mass of florencite grains, as analysed by microprobe, largely defined by hematite dusting in the plane light photo Fig 3 and by yellowish micromosaic (resembling alunite) in Xnic Fig 4, within fine quartz mosaic.

H/D/4** **Quartz-rich rock including quartz grains and areas of very fine-grained quartz, also masses of possible kaolinite with masses and lamellae of hematite. Small spherulites are texturally distinctive, their composition is optically Fe-stained kaolinite was identified by microprobe.**

Optically continuous grains of quartz with a poikilitic habit dominate this sample, with grains to 15mm or more in length. These are separated by areas of microcrystalline quartz, which contain limonite as irregular masses or along parallel planar fractures. Masses of microcrystalline, almost isotropic material also host similar limonite-filled fractures and masses and may be composed of kaolinite, although this is not entirely certain. Very minor hematite occurs as small crystals. In some areas of possible kaolinite ± limonite there are abundant disseminated small patches, typically circular or elliptical in outline, with a radial extinction pattern and a diameter of about 0.1mm. The mineral was examined briefly under the microprobe and is iron-stained kaolinite. A single grain of rhabdophane [$(Ce,La)PO_4.nH_2O$] was also identified by microprobe analysis.

Fig 5 **H/D/4** **0.09 mm**

PS. Part Xnic. Texturally distinctive spherulites, within a matrix of Fe-stained kaolinite. Microprobe analysis of this material did not indicate any REE content.

H/E/1** **Heterogeneous quartz-kaolinite (?)-limonite rock, with minor apatite > barite. Microprobe analysis of apatite and adjacent small grains contain Ce, P and Si and other REE.**

This is a heterogeneous rock with very irregular domains dominated by microcrystalline cherty quartz ± chalcedony, with other patches and domains apparently rich in microcrystalline possible kaolinite, with very minor disseminated quartz. Limonite occurs in various abundances in both types of domain. Large, partly limonite stained and veined crystals of apatite are disseminated (5-7%), to 3mm long and nearly 3mm wide. Small dense masses of limonite also occur, as well as small voids. Small grains of barite (1%) and rare quartz up to 1mm in diameter are rimmed by fine-grained quartz and limonite. Minor small grains adjacent to the apatite were found by microprobe analysis to contain abundant Ce, apparently as Ce^{4+}, but do not correspond to any known mineral. Other REE also occur in this mineral, as well as P and Si.

Fig 6 **H/E/1** **0.45 mm**
TS. PPL. Large central fractured apatite crystal. The Ce-rich microprobe analysis comes from within a fracture within this apatite crystal.

Fig 7 **H/E/1** **0.45 mm**
TS. Xnic. Partly altered (dark) apatite crystals within massive cryptocrystalline quartz and irregular zoning by dark equally fine hematite/limonite.

H/E/4 **Quartz-barite-limonite rock with are apatite, rare monazite/xenotime, also minor partly oxidised pyrite.**

Patches of granular barite occur irregularly through this sample (possibly 10-15%), but seem to have been partly leached, with remaining grains to 8mm long. Ribs of very fine-grained/microcrystalline quartz protrude into or separate the barite grains and large areas of similar quartz occur away from the barite masses. Among the coarser quartz grains (still <0.1mm grainsize), many have pale brown clouded cores and clear rims, but there are also variously clear and clouded small masses of fibrous quartz and/or chalcedony. Lenses and masses of coarser microsparry quartz are scattered, and there is a single crystal of apatite, 2mm long, stained and veined by limonite. Partly or completely limonitised pyrite occurs as grains and masses to 3mm long. Only rare small grains of monazite are disseminated, however, to 0.4mm in grainsize.

H/F/1 **Quartz-limonite rock with rare goethite and monazite, passing into zones with anastomosing or planar limonite-kaolinite lamellae, patches of quartz ± chalcedony. Minor lenses of monazite/xenotime and layers largely composed of barite.**

This sample can be divided into three zones:

Zone 1 has abundant microcrystalline quartz with limonite disseminated and in small planar laminae, mostly short, with lamellar or possibly fragmental textures in different areas. A single fan-like aggregate of goethite crystals is present as well as a single grain of monazite or xenotime.

Zone 2 has abundant irregularly anastomosing lamellae rich in limonite-clouded probable kaolinite to 2mm wide. These enclose areas of microcrystalline quartz, less limonite-stained than those in zone 1, but with planar or curved limonite plates possibly derived from hematite. Laminated limonite-quartz masses or fragments occur and there are sparse interstitial areas containing zones quartz-chalcedony-limonite patches. Along the margin of this zone there are lenses to 5mm long largely composed of granular monazite or xenotime, to 0.5mm grainsize, largely enclosed in essentially isotropic material, cryptocrystalline kaolinite or opal. The thin section may have 2-3% monazite.

Zone 3 has a layer 4mm wide with abundant barite as rounded grains to 4mm long, veined and separated by limonite ± microcrystalline quartz. Along the end of the thin section this passes into a foliated limonite-kaolinite band. Veins rimmed by chalcedony and filled with quartz cut across this zone.

H/F/3** **Heterogeneous massive barite-rich rock, with subordinate quartz, lesser kaolinite-muscovite-limonite-illite (?) aggregate. Minor hematite and monazite in patches and zones. Monazite analysed by microprobe and forms about 5% of this sample.**

Irregular masses of coarse granular barite are abundant in this sample (45-50% by volume) and as much as 25mm long. Zoned masses involving prismatic quartz, microsparry or microcrystalline quartz and chalcedony occur within and between the barite grains, with large areas of colloform-zoned silica (various types of quartz and chalcedony). There are also variously quartz-rich and clay-rich masses, with kaolinite and/or possible illite in the clay-rich areas, and areas rich in unoriented or spherulitic aggregates of muscovite to 2mm in diameter. Lenses of platy crystalline hematite (7-8%) also occur, to 8mm long, with rims of colloform quartz or chalcedony on the hematite, commonly facing into cavities filled with large optically continuous masses of quartz, rather than barite. Similar rims occur on nearby grains of barite, however, and there are lenses of granular monazite or xenotime to 0.8mm grainsize. One corner of the thin section contains a zone of massive granular monazite (analysed by microprobe) at least 5mm wide, with grains mostly less than 0.5mm and forms about 5% of this thin section.

Fig 8 **H/F/3** **0.18 mm**
TS. Xnic. Part of a large aggregate of monazite grains, with cleavage showing in some grains. [Black circled used for microprobe target location.]

Fig 9 **H/F/3** **0.09 mm**
TS. Xnic. High magnification of Fig 8 showing detail of monazite crystal aggregate with patches of cryptocrystalline silica partly crosscutting the monazite (bottom left quadrant) and opaque grains.

Figs 10 & 11 **H/F/3** **0.18 mm**

TS. Fig 9: PPL. Fig 10: Xnic. Central irregular pale infill of barite interstitial to complex mass of randomly interlocking blades of oxidised hematite with an immediate rim of clouded chalcedonic silica.

Fig 12 **H/F/3** **0.18 mm**

TS. Xnic. Aggregate of monazite crystals (coloured), and barite (pale-dark grey crystals left of monazite). Dark area to right of the monazite aggregate consists of supergene silver clays and hematite.

Fig 13 **H/F/3** **0.18 mm**

PTS. Reflected light (RL). Reflected light photo of Fig 12, particularly showing the dark areas above to consist largely of low temperature (?opaline or chalcedonic) silica and clays containing sparse disseminated extremely fine micaceous hematite.